J Mater Sci (2015) 50:906–922
DOI 10.1007/s10853-014-8651-z

Oxaprozin/poly(2-hydroxyethyl acrylate/itaconic acid) hydrogels: morphological, thermal, swelling, drug release and antibacterial properties

Marija M. Babić · Katarina M. Antić · Jovana S. Jovašević Vuković · Bojan Đ. Božić · Sladjana Z. Davidović · Jovanka M. Filipović · Simonida Lj. Tomić

Received: 31 July 2014 / Accepted: 4 October 2014 / Published online: 18 October 2014

Abstract In this study, a series of novel stimuli-sensitive hydrogels based on 2-hydroxyethyl acrylate and itaconic acid monomers were designed for the controlled release of hydrophobic drug, Oxaprozin. All samples were synthesized by the free-radical crosslinking copolymerization and characterized for structural, morphological, thermal, surface charge, swelling and antibacterial properties. In order to investigate the influence of the drug on hydrogel properties the same characterization was conducted for all Oxaprozin-loaded samples. The chemical composition of hydrogels was studied using Fourier transform infrared spectroscopy, while their morphology and thermal properties were examined by scanning electron microscopy and differential scanning calorimetry. Swelling studies, conducted in the physiological pH range from 2.20 to 8.00 and in the temperature range from 25 to 50 °C, showed that the loaded drug does not modify the pH and temperature sensitivity of the hydrogels, but reduces their swelling capacity. The in vitro drug release study conducted at pH 2.20 and 7.40 showed that all hydrogels can be tailored as colon specific drug delivery systems, and the drug release rate can be effectively controlled by IA content. In addition, the antibacterial activity of the hydrogels was determined against *Escherichia coli* and *Staphylococcus aureus*, by the zone of inhibition test. Results of our study indicate that these "smart" hydrogels, with specific morphology, surface charge, swelling capacity, drug loading efficiency and release behavior, could be designed to obtain an enhanced and site-specific controlled drug release system by simply adjusting their composition.

M. M. Babić · K. M. Antić · J. S. J. Vuković · B. Đ. Božić · S. Z. Davidović · J. M. Filipović · S. Lj. Tomić (✉)
Faculty of Technology and Metallurgy, University of Belgrade, Karnegijeva 4, Belgrade, Serbia
e-mail: simonida@tmf.bg.ac.rs

M. M. Babić
e-mail: mbabic@tmf.bg.ac.rs

K. M. Antić
e-mail: katarina.antic@tmf.bg.ac.rs

J. S. J. Vuković
e-mail: jjovasevic@tmf.bg.ac.rs

B. Đ. Božić
e-mail: bbozic@tmf.bg.ac.rs

S. Z. Davidović
e-mail: sdavidovic@tmf.bg.ac.rs

J. M. Filipović
e-mail: jfil@tmf.bg.ac.rs

Introduction

Hydrogels are three-dimensional (3D) cross-linked polymeric structures that possess excellent water retention capacity, and have soft tissue-like consistency [1]. Because of their non-toxicity, biocompatibility and biodegradability, hydrogels have attracted much attention as new biomaterials [2]. Their specific water-absorbing property makes them suitable for controlled drug delivery applications, wound-healing patches or films, cell encapsulation, tissue regeneration (bone, cartilage, skin, blood vessel, etc.), and for various biomedical and pharmaceutical applications [3–9].

Controlled drug release at the desired site of application is a critical and desirable behavior of a drug carrier which offers many advantages, including higher therapeutic efficacy with minimum side effects induced using a drug, patient compliance, as well as cost effectiveness of the drug regime over the conventional drug delivery systems

[10]. Although these systems have been in the research focus for a long time, they have not yet reached the high level of expectations. As a result, a new generation of drug formulations called self-regulated drug delivery systems have been introduced [11–14]. These systems are capable of recognizing changes in the parameters of normal physiological functions and act on them. Most of self-regulated drug delivery systems are based on "smart" hydrogels. The drug release profile from the hydrogel is generally influenced by many biological (pH, temperature, and biochemical microenvironment at the site of application) and physicochemical (functionality of polymer network) factors, which may, in turn, affect swelling, degradation, compression, and other properties important for a drug release [10, 15–18].

Temperature and pH-sensitive hydrogels could provide the ideal "smart" materials for the development of new controlled drug delivery systems. These hydrogels are able to release drug in a controlled manner in specific target regions of the body, in response to small changes of local pH and temperature values. Various natural and synthetic polymers have been used to make matrices, reservoir or implant devices, due to special properties of polymers, especially in regards to easiness of controlling biocompatibility, biodegradation, porosity, surface charge, mechanical strength and hydrophobicity/hydrophilicity [19, 20].

Poly(2-hydroxyethyl acrylate) (PHEA) is an interesting biomaterial [21–24] with similar biocompatibility and cell compatibility [25–27] as widely used poly(2-hydroxyethyl methacrylate) (PHEMA) [28]. However, it has been much less explored polymeric system for drug delivery applications. Since the PHEA hydrogels are non-ionic hydrogels, an improvement in the pH sensitivity and swelling capacity commonly requires modifying PHEA hydrogels by copolymerization with monomers containing ionic groups. Itaconic acid (IA) is highly hydrophilic monomer that has been recently studied in greater details in our laboratory to improve the swelling capacity, antimicrobial activity and biocompatibility of PHEMA hydrogels [29, 30]. In our previous research, hydrogels based on HEMA and IA were synthesized and characterized as controlled release systems of the antibiotics gentamicin sulfate and sodium sulfacetamide [46]. The PHEA and P(HEA/IA) hydrogels swell more than PHEMA and P(HEMA/IA) hydrogels, which were more investigated as sustained release controlled drug delivery systems. In both cases, dibasic IA easily copolymerizes and enriches the polymers chain with carboxylic side groups with different pK_a values, which in combination with higher hydrophilicity of HEA, is resulting in improved pH sensitivity and swelling capacity of P(HEA/IA) hydrogels. All hydrogels showed sustained release of drug.

In this study, a series of stimuli-sensitive hydrogels based on 2-hydroxyethyl acrylate and itaconic acid [PHEA and P(HEA/IA)] were synthesized and characterized for the controlled release. The aim was to design and develop suitable materials for an efficient and robust controlled drug delivery system, and also to evaluate the influence of loaded drug on their structure, morphological, thermal, swelling and antibacterial behavior. The drug release studies were conducted in vitro using oxaprozin (OXA), as active substance. Oxaprozin, 3-(4,5-diphenyl-1,3-oxazol-2-yl) propanoic acid is one of the leading non-steroidal anti-inflammatory drugs (NSAIDs) on US market, which is mainly used for the treatment of inflammatory musculoskeletal diseases, including rheumatoid arthritis, osteoarthritis, ankylosing spondylitis, tendinitis and bursitis [31]. However, the therapeutic benefits of NSAIDs are accompanied with several side effects including gastrointestinal injury, peptic ulceration and perforation [32], and major upper gastrointestinal hemorrhage. Several strategies have been proposed to control the critical side effects, but still there is no a pharmaceutical formulation that prevents the potential side effects completely [33]. The focus of our study is to development a novel, "smart" hydrogels as a potential controlled delivery system of OXA. These systems may provide controlled release at desired site with minimized side effects of the drug in upper gastrointestinal tract by reducing the concentration of the released drug into stomach.

Materials and methods

Materials

Monomers 2-hydroxyethyl acrylate (HEA, Sigma-Aldrich, 96.0 %) and itaconic acid (IA, Fluka, 99.6 %), were used as starting components for the hydrogel preparation. Ethylene glycol dimethacrylate (EGDMA, Aldrich, 97.0 %), potassium persulfate (KPS, Fluka, 99.0 %) and *N*, *N*, *N*′, *N*′-tetramethylene diamine (TEMED, Aldrich, 99.0 %) were used as a crosslinking agent, initiator and activator, respectively. The polymerization was performed in a mixture of water/ethanol.

Buffers with different pH values were prepared using following ingredients (analytical grade): hydrochloric acid (La Chema), potassium chloride (Fluka), potassium mono- and dihydrogenphosphate (Fluka) and sodium hydroxide (Fluka). Demineralized water was used for all polymerizations and the preparation of buffers. All materials used for synthesis of OXA were obtained from Aldrich and Fluka, and were used without further purification [35].

Synthesis of hydrogels

PHEA and P(HEA/IA) hydrogels were prepared by the free-radical crosslinking copolymerization, with IA mole fractions of 0.0, 2.0, 3.5, 5.0, and 7.0 (Scheme 1). Initiator,

Scheme 1 Synthesis of P(HEA/IA) hydrogels

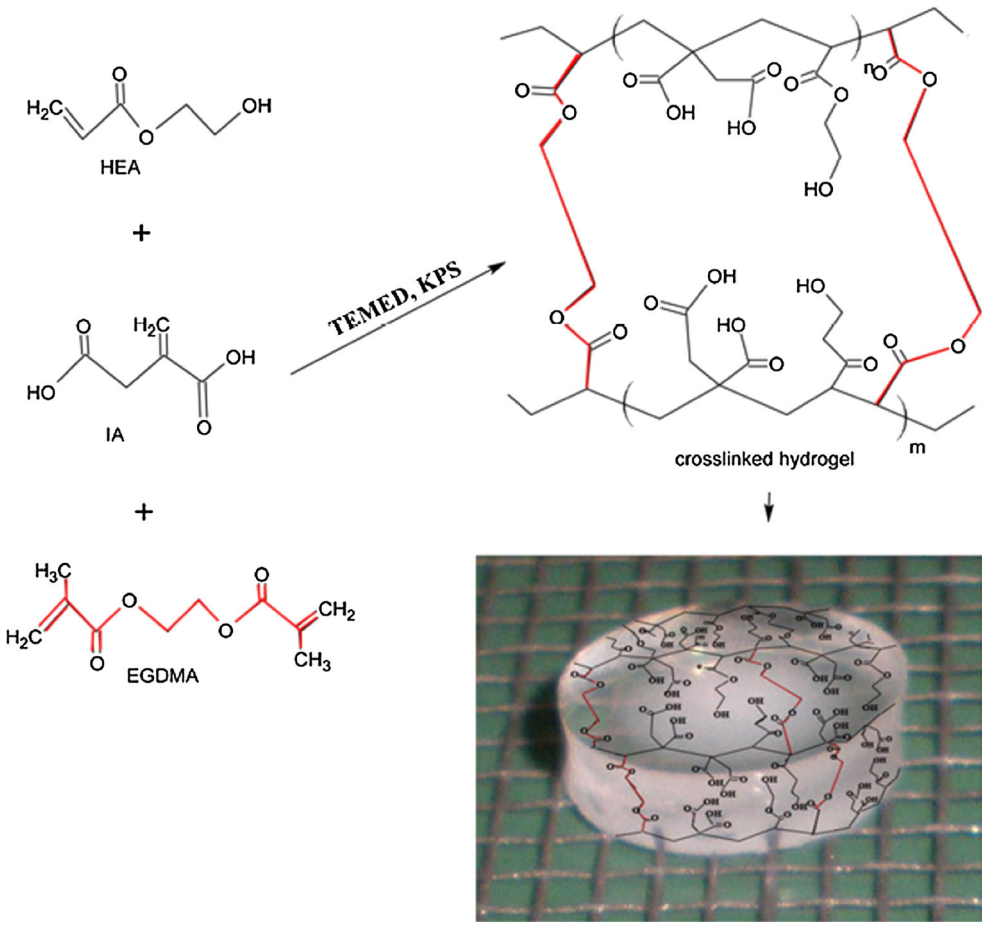

Table 1 Composition of PHEA and P(HEA/IA) hydrogels

	PHEA	P(HEA/2IA)	P(HEA/3.5IA)	P(HEA/5IA)	P(HEA/7IA)
HEA (mol%)	100	80	65	50	30
IA (mol%)	0	20	35	50	70

activator and crosslinker were added to the monomer feed (Table 1) previously dissolved in water/ethanol mixture, which was than purged with nitrogen and placed between two glass plates sealed with a rubber spacer (2 mm thick). Polymerization was carried out at 50 °C for 24 h. After the reaction, gels were cut into disks and immersed into water for a week, to remove unreacted components. Water was changed daily. After that, the disks were dried at ambient temperature to obtain xerogels. Unreacted monomers' concentration was determined using a UV spectroscopy, and by titration of extract against NaOH (0.05 mol/l) to phenolphthalein end-point, respectively. The results indicate that the conversion during crosslinking copolymerization was nearly complete, above 99 %. According to the IA mole fraction the samples were labeled as PHEA, P(HEA/2IA), P(HEA/3.5IA), P(HEA/5IA) and P(HEA/7IA), respectively.

Synthesis of Oxaprozin

Oxaprozin was synthesized according to the procedure described in the literature (Scheme 2) [35]. Characterization of the synthesized drug was performed accordingly [36]. Oxaprozin belongs to the Class II of the biopharmaceutics classification system (BCS), since it is a highly permeable but a very low soluble drug [34]. Drugs belonging to BSC II group are challenging for many researchers to develop suitable materials for drug carriers.

Fourier transform infrared spectroscopy (FTIR)

Drug-free and drug-loaded xerogels were crumbled into a powder and mixed with potassium bromide (Merck IR spectroscopy grade) in the proportion 1:100, and then

Scheme 2 Synthesis of Oxaprozin

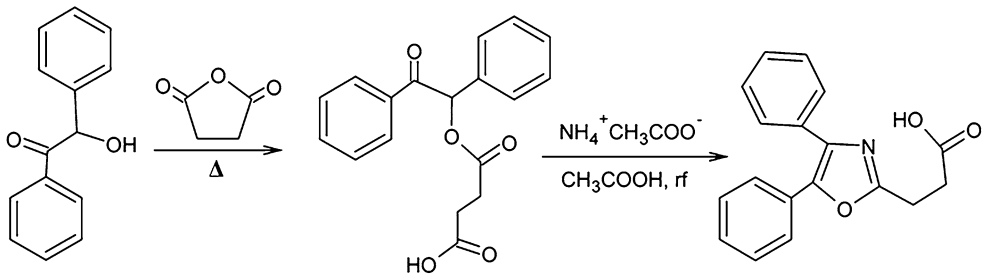

compressed into a 12-mm semi-transparent disk under a pressure (Pressure gage, Shimadzu). FTIR spectra over the wavelength range of 4000–700 cm^{-1}, were collected using a FTIR spectrometer (BOMEM Michelfan MB-102 FTIR, Canada).

Scanning electron microscopy (SEM)

A scanning electron microscope (JEOL JSM-5800 LV, USA) was used to observe specimen's morphologies. The samples were freeze-dried using a Modulyo Freeze Dryer System Edwards, consisting of a freeze dryer unit and a High Vacuum Pump E2M8. Before observation of morphology, xerogels were gold sputtered under vacuum.

Differential scanning calorimetry (DSC)

The glass transition temperatures of PHEA and P(HEA/IA) copolymeric networks were determined using a TA Instruments DSC Q2000 system (USA). The DSC was calibrated with metallic indium standards (99.9 % purity). The hydrogel samples were all desiccated at 40 °C for 24 h, and tested in crimped aluminum pans. The heating rate was 20 °C/min under nitrogen gas flow (50 mL/min). The test was conducted via two heating/cooling step cycles in the temperature range of −50 to 150 °C to eliminate any residual water. The glass transition was determined by the midpoint of the initial transition slopes.

Point of zero surface charge (PZC) analysis

The point of zero surface charge (pH_{PZC}) of drug-free, and drug-loaded PHEA and P(HEA/IA) hydrogels was measured according to the method described in the literature [37]. For the measurement of the pH_{PZC}, 40 ml of 0.1 N KNO_3 solution was transferred to series of 100-ml conical flasks. The initial pH of solutions (pH_i) was adjusted between 2 and 12 by adding 0.1 N HNO_3 or 0.1 N NaOH. The hydrogel samples were added to each flask, securely capped, and shaken thoroughly for 48 h to reach equilibrium at ambient temperature. The final pH values (pH_f) of the supernatant liquids were then measured. The difference between the initial and final pH values ($\Delta pH = pH_i - pH_f$) was plotted against the pH_i and the point of intersection of the obtained curve with pH_i abscissa, at which $\Delta pH = 0$, indicated the pH_{PZC} value of an investigated hydrogel.

Swelling studies

Dynamic swelling measurements were carried out in buffers mimicking biological fluids, in a pH range of 2.20, 3.85, 4.50, 5.45, 6.20, 6.80, 7.40 and 8.00, and in a temperature range from 25 to 50 °C. The amount of fluid absorbed as a function of time was monitored gravimetrically. Swollen gels were removed from the swelling medium at regular intervals and dried superficially with filter paper. They were then weighed and placed in the same bath until a constant weight was reached for each sample. The equilibrium degree of swelling (q_e) was calculated as follows:

$$q_e = \frac{m_e - m_o}{m_o} \quad (1)$$

where m_e is the weight of a swollen hydrogel at equilibrium, and m_o is the weight of a xerogel [38, 39]. All the swelling experiments were performed in triplicate.

Swelling behavior of hydrogels, were also studied under simulated gastrointestinal conditions. Drug-free and drug-loaded xerogels were initially swollen in the simulated stomach conditions (pH 2.20), and after 2 h (gastric transit time) were transferred to the small intestine conditions (pH 6.80) where they were kept for 6 h (small intestine transit time). Subsequently, they were transferred to colon conditions (pH 8.00) for 12 h (colon transit time). At regular time intervals, samples were removed from the swelling medium, blotted with filter paper and weighed. All the swelling experiments were performed in triplicate.

To investigate diffusion properties of the hydrogel, kinetic parameters were calculated using following equation [40]:

$$\frac{M_t}{M_e} = kt^n \quad (2)$$

where M_t and M_e are fluid absorbed at time t and at the equilibrium, respectively; k is the kinetic constant related

Table 2 Kinetics models and equation used to fit experimental drug release data

	Kinetic model	Equation	Parameters
1.	Higuchi equation—describes the Fickian diffusion of drug [43]:	$F = k_H t^{1/2}$ (6)	Where F is the fractional drug release, k_H is kinetic constant and t is the release time
2.	Ritger–Peppas equation	$F = k_1 t^n$ (7)	Where F is the fractional drug release, k_1 is kinetic constant, t is the release time and n is the diffusional exponent
3.	Peppas–Sahlin equation, which accounts for the coupled effects of Fickian diffusion and Case II transport [44]	$F = k_1 t^m + k_2 t^{2m}$ (8)	The first term of this equation represents the contribution of Fickian diffusion and the second term refers to the macromolecular relaxation contribution on the overall release mechanism
4.	Peppas–Sahlin equation where exponent m fixed to 0.5	$F = k_1 t^{1/2} + k_2 t$ (9)	Where F is the fractional drug release, k_1 and k_2 are kinetic constants, and t is the release time

to the structure of the network, and n is the diffusion exponent. Logarithmic form of Eq. 2 was used to calculate n and k from the slope and intercept, respectively, from the linear parts of the swelling curves of drug-free and drug-loaded hydrogels. The diffusion coefficient, (D), was calculated from the following equation [41]:

$$D = k^{1/n}\pi\frac{l^2}{16} \tag{3}$$

where l is the thickness of the xerogel.

Drug loading and entrapment efficiency

OXA was loaded in hydrogels by a diffusion method. The PHEA and P(HEA/IA) xerogels were swollen in 10 ml of Oxaprozin solution in a buffer of pH 8.00 to reach equilibrium and allowing enough time for the drug to diffuse into the gel. Higher pH of a buffer was selected as optimal drug loading conditions, in which the drug showed good solubility and the hydrogels higher swelling capacity. After 48 h of swelling, the swollen hydrogels were carefully taken out from the drug solution and washed with the same solution to remove free drug particles from the samples. The solution was then analyzed using an UV spectrophotometer (Shimadzu UV/Vis Spectrophotometer UV-1800, Japan) to determine the amount of unloaded OXA (at $\lambda = 284$ nm). This value was then compared to the total amount of added OXA to determine the Oxaprozin-entrapment efficiency of the hydrogels [42]. Finally, the swollen hydrogels were dried at ambient temperature for several days to constant mass and used for the release experiments.

The drug loading (DL) and entrapment efficiency (EE %) of the hydrogels were calculated by the following equations:

$$\mathrm{DL(mg/g\ hydrogel)} = \frac{\text{(weight of drug in hydrogel)}}{\text{(weight of drug free xerogel)}} \tag{4}$$

$$\mathrm{EE\ (\%)} = \frac{\text{(content of drug in hydrogel)}}{\text{(theoretical content of drug)}} \times 100 \tag{5}$$

In vitro controlled drug release study

In vitro Oxaprozin release behavior of P(HEA) and P(HEA/IA) hydrogels were investigated at low and high pH values to verify release potential, and confirm the pH-dependent delivery. Drug-loaded disks were evaluated for OXA release by placing the disk in a basket stirrer containing 10 ml of release medium, at 37 ± 0.5 °C. The release media were buffers of pH 2.20 (simulated gastric conditions) and 7.40 (simulated intestine/colon conditions). The rotation speed was 50 ± 1 rpm. The amount of OXA released was measured spectrophotometrically, using a UV spectrophotometer (Shimadzu UV/Vis Spectrophotometer UV-1800, Japan) by taking the absorbance of the solution containing released drug at regular time intervals, at wavelength of 284 nm. The concentration of released drug was determined using a calibration curve. All release experiments were carried out in triplicates.

Analysis of the drug transport mechanism

To evaluate the release kinetics, the first 60 % of the drug release data of PHEA and P(HEA/IA) hydrogels were fitted to the well-known kinetic models, such as the Higuchi model, Ritger-Peppas, Peppas-Sahlin and Peppas-Sahlin model when $m = 0.5$ (Table 2).

Using the estimated parameters k_1 and k_2 obtained from fitting the experimental release data to Eq. 9 (Table 2), the

ratio of relaxation (R) and Fickian (F) contributions was calculated using the following equation:

$$\frac{R}{F} = \frac{k_2}{k_1} t^{1/2} \tag{10}$$

Experimental data were analyzed by a nonlinear least-squares regression. The sum of the squared residuals (SSR) and Akaike Information Criterion (AIC) was determined for each model as indicators of the model suitability for obtained data set. The model that shows the smallest value for the AIC best describes drug release mechanism [45].

Antibacterial assay

The antibacterial activity of the drug-free and drug-loaded P(HEA/IA) hydrogels was screened using the zone of inhibition test due to fact that hydrogels containing IA, which is obtained from natural renewable sources, could be considered as a good barrier against the microbes. On the other hand, a variety of pharmaceutical preparations, which are applied in the management of non-infectious diseases, have shown in vitro some antimicrobial activity. These drugs are called "non-antibiotics". Oxaprozin belongs to these drugs due to its features to inhibit growth of the *Pseudomonas aeruginosa* [60].

The antibacterial activity was tested against pathogenic Gram-negative *Escherichia coli* (ATCC 25922) and Gram-positive *Staphylococcus aureus* (ATCC 25923) bacteria. The inoculum of the microorganism was prepared in a sterile physiological saline solution (8.5 g NaCl in 1 L of distilled water) to obtain ca. 10^5 CFU/mL. The tryptone soy broth (Torlak) with 0.6 % yeast extract (TSBY) was added as a growing medium. Afterwards, the suspension was vortexed and poured in Petri dishes over layered with tryptone soy agar (TSAY). After that, the swollen hydrogel samples were placed onto the surface of inoculated agar dishes and incubated at 37 °C for 24 h. The weights of drug-free PHEA, P(HEA/2IA) and P(HEA/7IA) hydrogel were 0.2002, 0.3100 and 0.4955 g, respectively. The weights of drug-loaded PHEA, P(HEA/2IA) and P(HEA/7IA) hydrogel were 0.1924, 0.2842 and 0.4200 g, respectively. As a control sample, pure agar solution without sample was used. Following incubation, the antibacterial activity was examined in regards to the zone of inhibition properties. All analyses of antibacterial activity were performed in triplicate.

Results and discussion

Fourier transform infrared (FTIR) spectroscopy

FTIR spectroscopic analysis was used to illustrate the chemical composition and the nature of bond formation into the hydrogels. The incorporation of IA and HEA monomers and drug in hydrogels was also confirmed using FTIR spectroscopy. The FTIR spectra for drug-free and drug-loaded PHEA, P(HEA/2IA) and P(HEA/7IA) hydrogels are presented in Fig. 1.

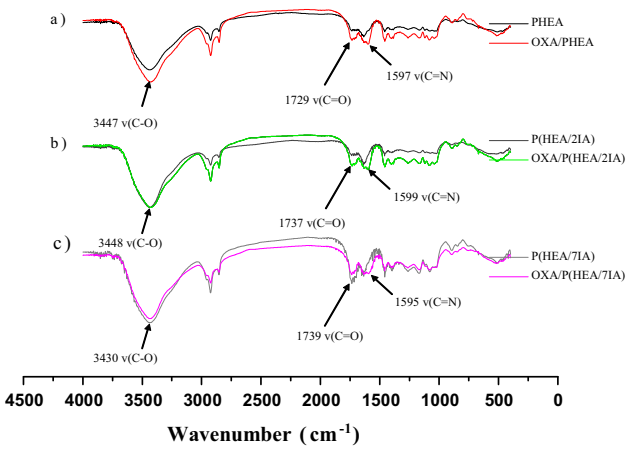

Fig. 1 FTIR spectra of drug-free and drug-loaded PHEA, P(HEA/2IA) and P(HEA/7IA) hydrogels

In the FTIR spectrum of PHEA, the observed peaks are assigned as follows: the characteristic peak of OH group at 3447 cm^{-1} (C–O stretching), the ester peak at 1729 cm^{-1} (C=O stretching) and aliphatic peaks in the range of 2900–3000 cm^{-1} (C–H stretching). The increased peaks intensity of the C = O group at 1737 cm^{-1} in the spectra of P(HEA/2IA) and OXA/P(HEA/2IA), and at 1739 cm^{-1} in the spectra of P(HEA/7IA) and OXA/P(HEA/7IA) were associates with the presence of the additional C=O groups from IA and OXA. Spectra of P(HEA/2IA) and P(HEA/7IA) samples show a broader peak in the range of 3700–3100 cm^{-1} which is the evidence of the OH stretching vibrations of carboxylic groups of IA [46]. The typical peaks of OXA (C=N stretching) at 1597, 1599 and 1595 cm^{-1} were observed in spectrum of OXA/PHEA, OXA/P(HEA/2IA) and OXA/P(HEA/7IA) samples which confirms successful incorporation of OXA in a hydrogel matrix [47].

Morphology

Morphological studies were performed to examine surface and cross-sectional part of xerogels by SEM. SEM micrographs are presented in Fig. 2.

SEM micrographs revealed that hydrogels prepared without IA (Fig. 2a) indicate compact, smooth and dense surface while hydrogels with higher content of IA (Fig. 2b) showed wavy, corral-like texture, with microchannels. The morphology of the surface of P(HEA/7IA) xerogel is changed to less wavy surface after loading of OXA (Fig. 2d) due to microchannels that were filled with OXA

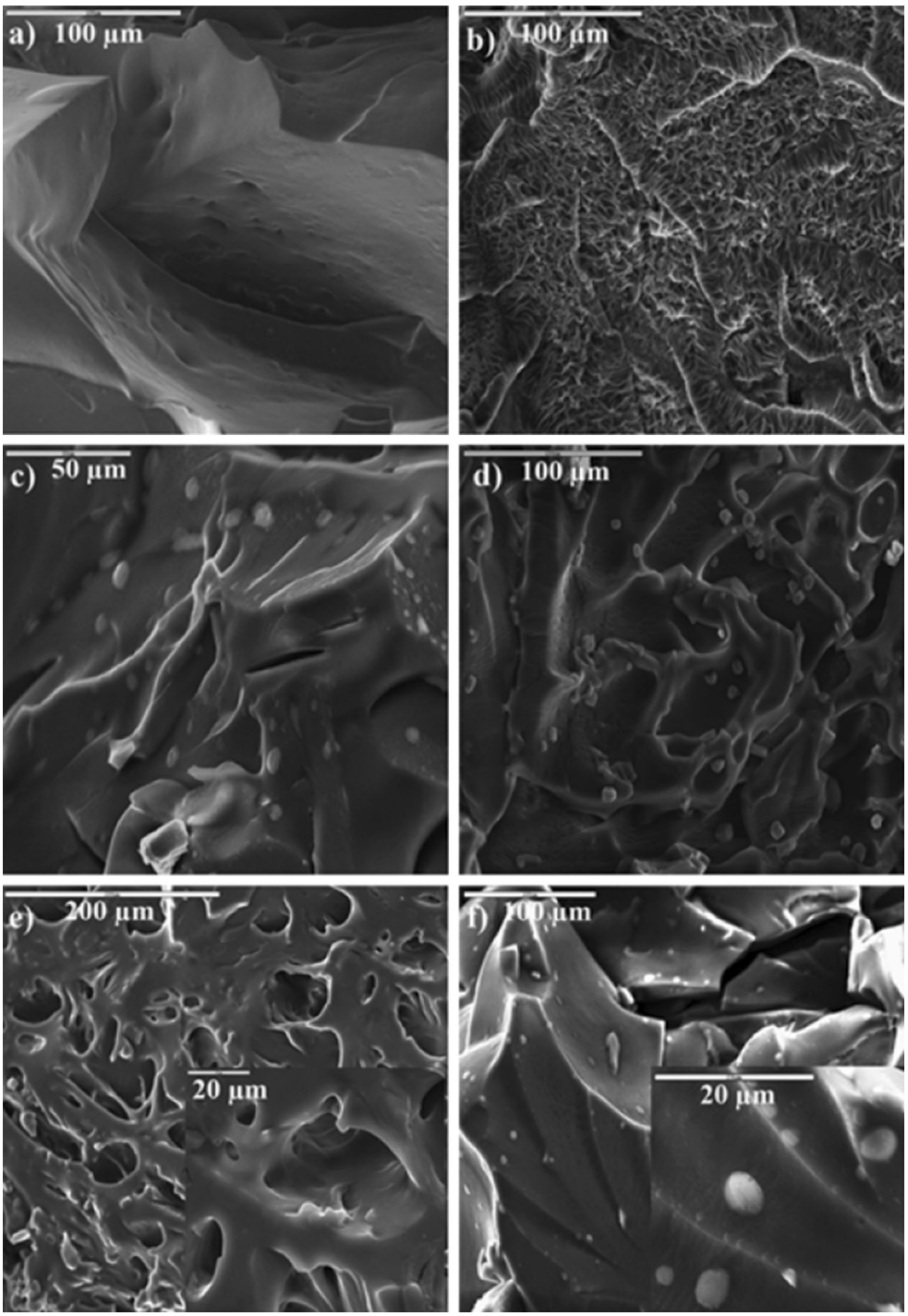

Fig. 2 SEM micrographs of surface morphology of **a** PHEA, **b** P(HEA/7IA), **c** OXA/PHEA, **d** OXA/P(HEA/7IA) and of cross-section morphology of **e** P(HEA/7IA) and **f** OXA/P(HEA/7IA) xerogels

particles. SEM images of the cross-section of P(HEA/7IA) xerogels (Fig. 2e) revealed distinct, heterogeneous porous structure, compared to the drug-loaded P(HEA/7IA) xerogel (Fig. 2f). OXA/P(HEA/7IA) exhibits less porous structure, with isolated smaller particles and some aggregates of OXA distributed throughout the interior. The observed morphological studies show that morphology of xerogels was changed by the presence of OXA, confirming a successful drug incorporation into PHEA and P(HEA/IA) hydrogels.

Thermal properties

Differential scanning calorimetry was used to determine the glass transition temperature (T_g) of drug-free and drug-loaded PHEA and P(HEA/IA) hydrogels. For all copolymeric networks a single T_g value was clearly observed, indicating that all the samples are indeed copolymers. Besides, there is a clear dependence of T_g value on the copolymer composition. The observed glass transition temperatures of drug-free PHEA, P(HEA/2IA), P(HEA/3.5IA), P(HEA/5IA) and P(HEA/7IA) hydrogels were 15, 22, 25, 30 and 34 °C, respectively. The drug-loaded PHEA, P(HEA/2IA), P(HEA/3.5IA), P(HEA/5IA) and P(HEA/7IA) hydrogels show T_g values of 20, 28, 32, 40 and 45 °C, respectively.

The T_g values for P(HEA/IA) copolymers are higher than those of PHEA due to the presence of IA residues. The T_g values for drug-loaded copolymers are higher than those for drug-free copolymers due to the incorporation of the drug into pores, reducing the mobility of polymeric chains. Melting point of OXA is 158–159 °C. The thermograms of drug-loaded polymeric networks showed a single T_g transition and no melting peak of OXA was observed. The results suggested that OXA is highly dispersed in the polymeric network.

Point of zero charge (PZC) analysis

Testing the surface charge of hydrogels is a very important for their drug delivery application. Not only the drug loading efficiency of hydrogels and their release rate are affected, but also adsorption into body membranes is significantly altered by surface charge of hydrogels. Strong anionic charge on the polymer surface is one of the required characteristics for mucoadhesion [61] which is very important for drug delivery to specific site in the body. Suitable surface charge of hydrogel can improve drug release profiles to specific site, reduce side effects of drug and improve therapeutic efficacy and patient compliance.

The point of zero surface charge of a hydrogel is the pH value (pH_{PZC}) at which negative and positive surface charge of a hydrogel are equal, $pH_{PZC} = 0$. Depending on the pH of the ambient solution, the surface charge of a hydrogel will have negative value for $pH > pH_{PZC}$, positive for $pH < pH_{PZC}$, or neutral for $pH = pH_{PZC}$ [48]. The variation in ΔpH as a function of pHi in 0.1 N KNO3 as a background electrolyte are presented in Fig. 3 for drug-free and drug-loaded (a) PHEA, (b) P(HEA/3.5IA) and (c) P(HEA/7IA) hydrogels.

PHEA and P(HEA/IA) hydrogels have pH-dependent surface charge due to the presence of ionic groups on their surfaces, which can be ionized or deionized depending on the pH of the ambient solution. As expected, the measured pH_{PZC} values depend on the surface composition of hydrogels. The drug-loaded hydrogels show the same value of pH_{PZC} and all samples indicate neutral surface charge at pH around 7. We found that the drug has no effect on the surface charge of PHEA hydrogel, but it leads to changes in the pH_{PZC} values of the hydrogels containing itaconic acid. Adsorption of OXA on hydrogels containing IA, increases the negative charges on their surfaces. As a result, the pH_{PZC} values of P(HEA/3.5IA) and P(HEA/7IA) hydrogels

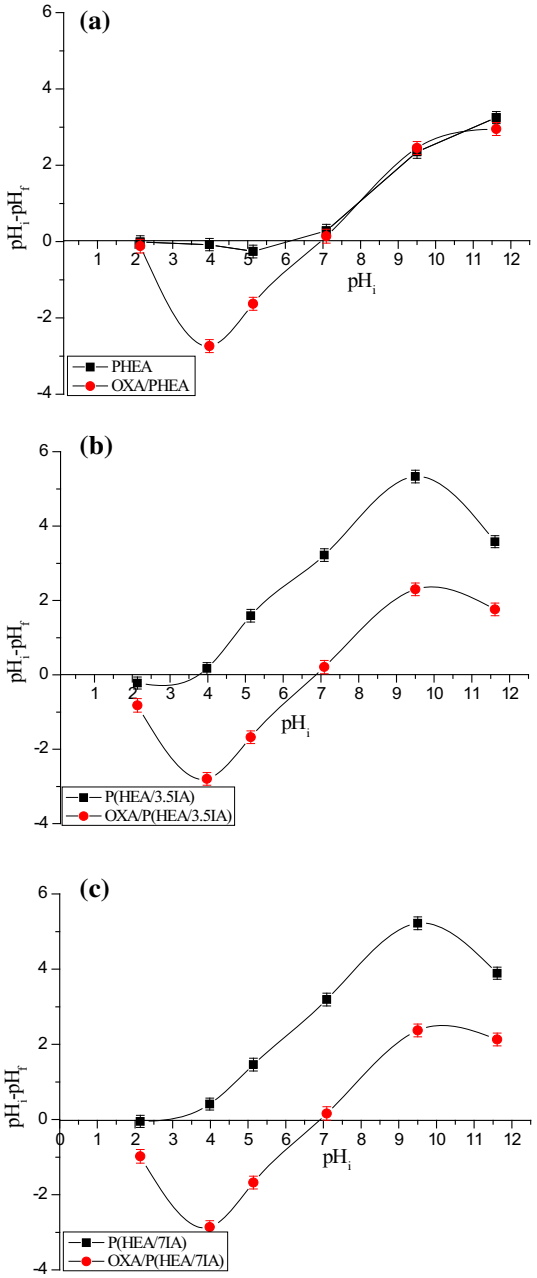

Fig. 3 PZC analysis of drug-free and drug-loaded **a** PHEA, **b** P(HEA/3.5IA) and **c** P(HEA/7IA) hydrogels

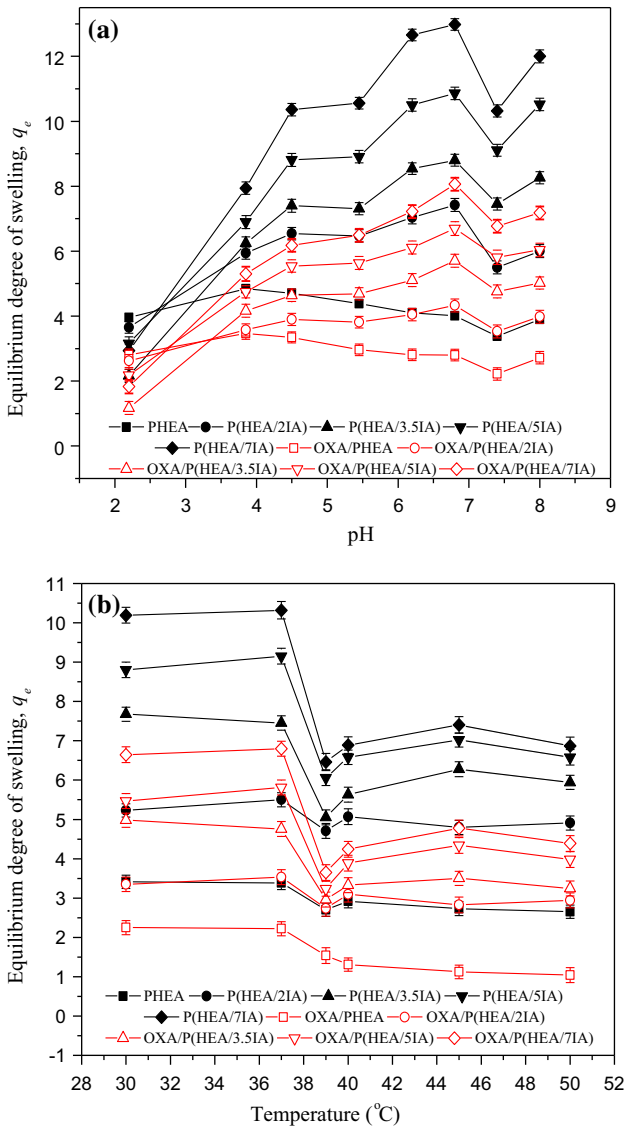

Fig. 4 **a** pH- and **b** temperature-sensitive swelling behavior for drug-free and drug-loaded PHEA and P(HEA/IA) hydrogels

shifted from 4 to 7 and from 3 to 7, respectively. This is in accordance with the fact that the specific sorption of anions shifts the pH_{PZC} toward higher pH values [49].

Swelling study

One of the most important characteristic of pH- and temperature-sensitive hydrogels for the drug delivery applications is the swelling capacity of the hydrogels, since this property could modulate the delivery profiles of bioactive molecules [50]. Also, the extent of hydrogel swelling is a critical parameter for a list of medical applications where the hydrogel-based devices may be implanted in a close proximity of nerves, blood vessels, or other pressure-sensitive body organs (i.e. spine or brain surgery applications). In this study, the swelling experiments were performed in the pH range of 2.20–8.00, at 37 °C, as well as in temperature range of 25–55 °C for selected conditions. Equilibrium degree of swelling (q_e) of drug-free and drug-loaded hydrogels as a function of pH and temperature are presented in Fig. 4a, b.

As clearly indicated in Fig. 4a, P(HEA/IA) hydrogels are pH-sensitive. The pH dependences of equilibrium degree of swelling (q_e) exhibit similar trend for all samples. At pH below pK_a values of IA groups ($pK_{a1} = 3.85$ and $pK_{a2} = 5.45$), the degree of swelling is low for all hydrogel samples. This is because carboxylic groups are not ionized, and thus form intramolecular hydrogen bonds, which in turn, results in the more compact network structure. As the pH value of the surrounding medium raises above pK_a values of both carboxylic groups, the electrostatic repulsive forces among the carboxylic anion groups become dominant, leading to the more expanded polymeric network structure and consequently to higher q_e values. The drug-free and drug-loaded PHEA hydrogels are not pH-sensitive, because the HEA monomer is neutral. PHEA and P(HEA/IA) hydrogel samples exhibit higher q_e values, compared to the corresponding samples containing the drug. The mobility and relaxation of the polymeric chains are hindered by the loaded drug, which decreases available free network space, resulting in lower q_e values.

The temperature sensitivity of the hydrogels was also studied via their swelling behavior (Fig. 4b). We found that the q_e decreases suddenly in the temperature range from 37 to 39 °C suggesting that P(HEA/IA) hydrogels are temperature sensitive. The volume phase transition temperature (VPTT) of these hydrogels is around 39 °C, which is in the physiologically relevant interval. The hydrogels showed high q_e values at temperature below the VPTT, and low q_e at temperature above the VPTT. At temperatures below the VPTT, the strong hydrogen bonding interactions between the hydrophilic groups of polymer and water molecules are responsible for the expansion of the polymeric network, resulting in higher q_e. Therefore, at temperatures above the VPTT, intramolecular interactions (polymer–polymer and/or water–water) became stronger, while the intermolecular (polymer-water) interactions are significantly reduced expelling the water from the hydrogel matrix. This leads to a change in hydrophilic character of hydrogels to hydrophobic, causing the hydrogels to swell less. Obtained swelling results indicate that P(HEA/IA) hydrogels are pH- and temperature-sensitive. In addition, the loading of OXA does not alter their pH and temperature sensitivity, but only reduces their swelling capacity.

Swelling behavior in simulated gastrointestinal condition

The swelling results obtained in simulated gastrointestinal conditions are presented in Fig. 5a for drug-free and in

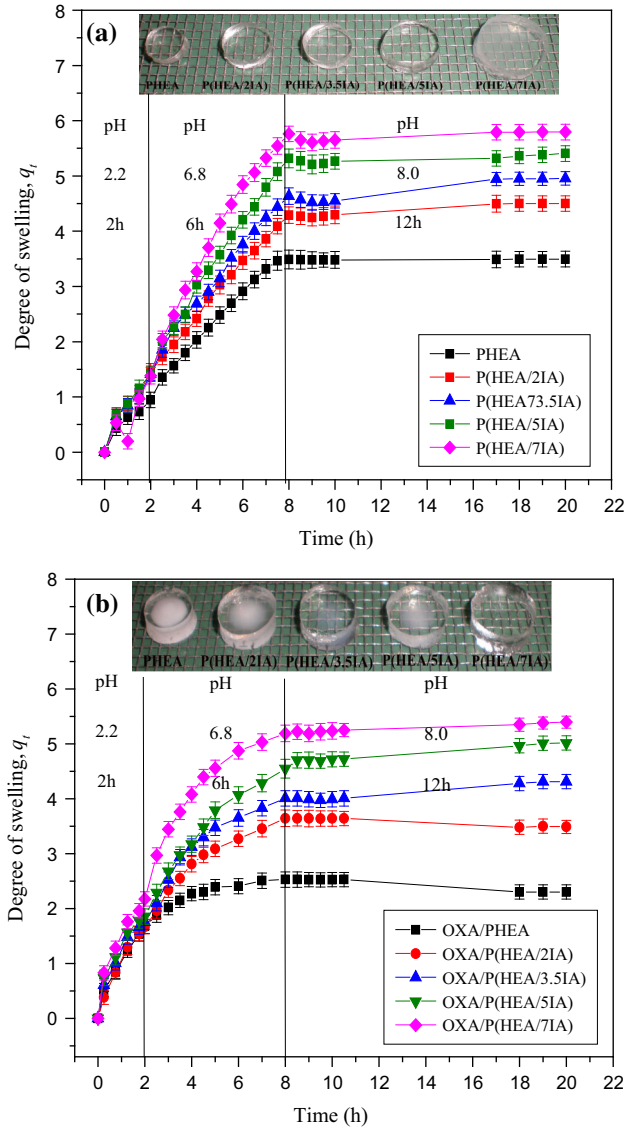

Fig. 5 Swelling behavior of **a** drug-free and **b** drug-loaded PHEA and P(HEA/IA) hydrogels in simulated gastrointestinal condition

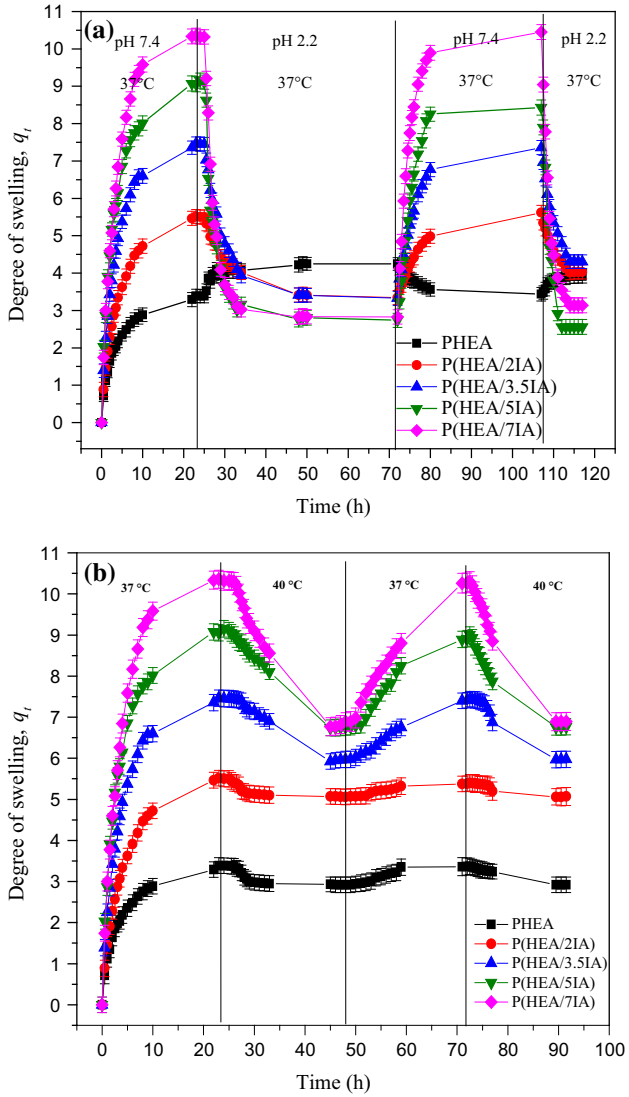

Fig. 6 Swelling–deswelling behavior of PHEA and P(HEA/IA) hydrogels under varying **a** pH and **b** temperature conditions

Fig. 5b for drug-loaded PHEA and P(HEA/IA) hydrogels. Photographs of the drug-free and drug-loaded hydrogels after swelling in simulated gastrointestinal conditions are also included in Fig. 5a, b.

As shown in Fig. 5a, b, the values of q_e are low at pH of 2.20 but they significantly increase when the samples were transferred to higher pHs 6.80 and 8.00. The swelling rate of OXA loaded hydrogels is slower compared to that of the drug-free counterpart. The lower swelling capacity of PHEA and P(HEA/IA) hydrogels in acidic pH, and higher swelling capacity in slightly alkaline pH, very advantageous for design of a colon specific drug delivery systems. These systems are also highly suitable for drug carriers of active agents that are generally unstable in harsh gastric environment.

Oscillatory swelling–deswelling study

The swelling–deswelling reversibility of PHEA and P(HEA/IA) hydrogels under oscillatory pH (of 7.40 and 2.20) and temperature (37–40 °C) were investigated to confirm the reversibility and response rate of the swelling process. This behavior is important to control drug release by a feed-back mechanism [51, 52]. Results on swelling–deswelling reversibility under pH and temperature varying conditions are presented in Fig. 6a, b.

Data in Fig. 6 indicate that P(HEA/IA) hydrogels showed excellent swelling–deswelling reversibility. It is evident that the swelling rate of samples is much slower than deswelling rate. This is due to the fact that under these conditions, a fluid can easily expel from swollen network structure, while the diffusion of a fluid into the network

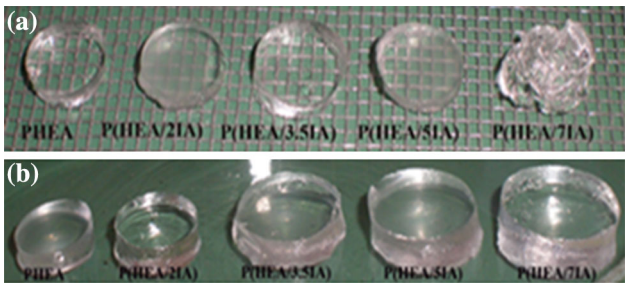

Fig. 7 Hydrogels samples after second cycle swelling–deswelling in **a** pH changes and **b** temperature change

structure is more hindered by the shrunken polymeric chains and pores. We also found that addition of IA in hydrogels improves their pH- and temperature reversibility. The P(HEA/7IA) hydrogel showed the best pH reversibility and rapid response rate but a rather poor strength; after the second cycle of pH changes, the hydrogel was cracked (Fig. 7a). In the case of varying temperature in pH of 7.40, the hydrogels show reversible symmetrical swelling–deswelling behavior between temperatures of 37 and 40 °C (temperature below and above the VPTT of hydrogels). All samples retained their strength after the second cycle of varying temperatures. Photographs of these hydrogels are presented in Fig. 7b.

Diffusion kinetics

The values of equilibrium degree of swelling, q_e, diffusion exponent, n, kinetic constant, k, and diffusion coefficient, D, for drug-free and drug-loaded PHEA and P(HEA/IA) hydrogels, in a buffer pH of 7.40, at 37 °C, are listed in Table 3.

Different mechanisms, based on the parameter n, can be used to describe the solvent and solute transport through a polymeric network. The transport mechanism can be Fickian ($n \leq 0.5$), non-Fickian, or anomalous ($0.5 < n < 1$). It can also represent Case II transport ($n = 1$) or Super-case II transport ($n > 1$) [53]. Obtained values of n for drug-free hydrogels are in range from 0.49 to 0.64, and for drug-loaded from 0.48 to 0.67. This indicate that the fluid transport mechanism is the Fickian diffusion for drug-free and drug-loaded PHEA, P(HEA/2IA) and P(HEA/3.5IA) but non-Fickian for drug-free and drug-loaded P(HEA/5IA) and P(HEA/7IA). It means that both, diffusion and relaxation of polymeric chains control the transport of fluid trough P(HEA/5IA) and P(HEA/7IA) hydrogels. The values of the diffusion coefficient increase with increasing IA content, but slightly decrease with loaded OXA, which is in accordance with a swelling capacity of hydrogels discussed earlier in the text.

Network parameters

The important structural parameters of the hydrogels are the average molecular weight of the polymeric chain between the two neighboring crosslinking points ($\bar{M}_c$), the effective crosslinking density (v_e) and pore size (ξ). The molecular weight between the crosslinks, for ionic hydrogels is calculated using the following equation [54]:

Table 3 Values of the equilibrium degree of swelling, q_e, diffusion exponent, n, kinetic constant, k, and diffusion coefficient, D, for drug-free and drug-loaded PHEA and P(HEA/IA) hydrogels, in a buffer pH of 7.40, at 37 °C

Sample	q_e		n		k (s^{-1})		$D \times 10^7$ ($cm^2\ s^{-1}$)	
	Drug free	Drug loaded	Drug free	Drug loaded	Drug free	Drug loaded	Drug free	Drug loaded
PHEA	3.38	2.22	0.49	0.48	0.33	0.44	1.37	1.32
P(HEA/2IA)	5.50	3.53	0.48	0.49	0.30	0.51	1.47	1.41
P(HEA/3.5IA)	7.45	4.76	0.49	0.45	0.33	0.52	1.53	1.48
P(HEA/5IA)	9.11	5.81	0.58	0.67	0.32	0.40	1.91	1.88
P(HEA/7IA)	10.32	6.77	0.64	0.67	0.28	0.44	1.92	1.89

Table 4 The calculated network parameters of drug-free and drug-loaded PHEA and P(HEA/IA) hydrogels, in pH of 7.40 and at 37 °C

Sample	q_e		$\bar{M}_c$ ($g\ mol^{-1}$)		V_e ($mol\ dm^{-3}$)		ξ (nm)	
	Drug free	Drug loaded	Drug free	Drug loaded	Drug free	Drug loaded	Drug free	Drug loaded
PHEA	3.38	2.22	5895	2152	0.168	0.460	7.146	4.317
P(HEA/2IA)	5.50	3.53	16839	5806	0.058	0.169	13.47	7.913
P(HEA/3.5IA)	7.45	4.76	35635	11727	0.027	0.083	21.15	12.13
P(HEA/5IA)	9.11	5.81	58336	18949	0.164	0.051	28.54	16.26
P(HEA/7IA)	10.3	6.77	77920	27448	0.012	0.035	34.10	20.24

$$\frac{V_1 X^2 \phi_{2,s}^2}{4I\bar{V}_r^2}\left(\frac{2K_{a1}K_{a2}+10^{-pH}K_{a1}}{2(10^{-pH})^2+10^{-pH}K_{a1}+K_{a1}K_{a2}}\right)^2 = \left[\ln(1-\phi_{2,s})+\phi_{2,s}+\chi\phi_{2,s}^2\right]+\left(\frac{V_1\rho}{\bar{M}_c}\right)\phi_{2,r}^{2/3}\phi_{2,s}^{1/3} \quad (11)$$

where K_{a1} and K_{a2} are the first and second dissociation constants of a diprotic acid, X is the weight fraction of ionisable polymer in the system, I is ionic strength of the swelling medium, $\phi_{2,s}$ is the polymer volume fraction in the swollen gel, $\phi_{2,r}$ is the polymer volume fraction in the relaxed state, V_1 is the molar volume of water, ρ is the polymer density, $\bar{V}_r$ is the average molar volume of polymer repeating units, and χ is the Flory polymer–solvent interaction parameter. The effective crosslinking density (v_e) was calculated as:

$$v_e = \rho\sqrt{M_c} \quad (12)$$

The network pore size (ξ) represents the distance between consecutive crosslinking points, which describes the available space for solute transport within the polymeric network, was calculated according to equation [55]:

$$\xi = \phi_{2,s}^{-1/3} l\left(\frac{2C_n\bar{M}_c}{M_r}\right)^{1/2} \quad (13)$$

Here M_r is the molecular weight of the repeating unit, l is the C–C bond length and C_n is the Flory characteristic ratio [56].

Experimental data of the swelling experiments conducted in a pH of 7.40 and at 37 °C were used for network parameters determination of drug-free and drug-loaded PHEA and P(HEA/IA) hydrogels. These data are shown in Table 4.

We found that the values of effective crosslinking densities (v_e) for drug-free hydrogels are in the range of 0.168–0.012 mol dm^{-3}, and for drug-loaded hydrogels are in range of 0.460–0.035 mol dm^{-3}. Drug-loaded hydrogels showed higher values of crosslinking densities compared to the drug-free hydrogels. The pore size (ξ) is one of the important hydrogel parameters that influences drug loading efficacy and release properties from hydrogels. We would like to emphasize that the pore size and molecular weight between two crosslinks increase with increasing of IA content.

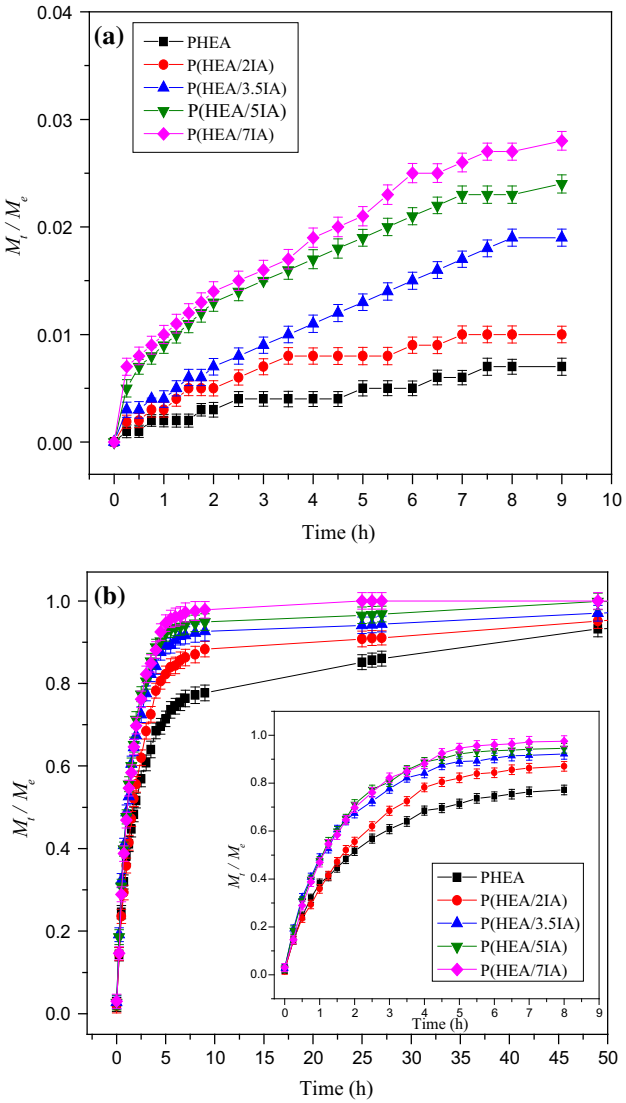

Fig. 8 In vitro release profiles of OXA from PHEA and P(HEA/IA) hydrogels in **a** pH of 2.20 and **b** pH of 7.40, at 37 °C

Table 5 Weight of xerogels, concentration of initial OXA solution, concentration of OXA solution after loading, loading (DL) and entrapment efficiency (EE) of PHEA and P(HEA/IA) hydrogels

Sample	Weight of xerogels (g)	Concentration of OXA solution before loading (mmol dm^{-3})	Concentration of OXA solution after loading (mmol dm^{-3})	DL ($mg_{drug}/g_{hydrogel}$)	EE (%)
PHEA	0.0515 ± 0.001	0.44 ± 0.001	0.25 ± 0.002	22 ± 0.11	42 ± 0.12
P(HEA/2IA)	0.0500 ± 0.001	0.43 ± 0.001	0.20 ± 0.002	27 ± 0.12	53 ± 0.12
P(HEA/3.5IA)	0.0494 ± 0.002	0.43 ± 0.001	0.16 ± 0.003	32 ± 0.11	62 ± 0.13
P(HEA/5IA)	0.0544 ± 0.002	0.46 ± 0.002	0.14 ± 0.003	35 ± 0.13	70 ± 0.14
P(HEA/7IA)	0.0508 ± 0.002	0.43 ± 0.002	0.11 ± 0.003	37 ± 0.13	75 ± 0.14

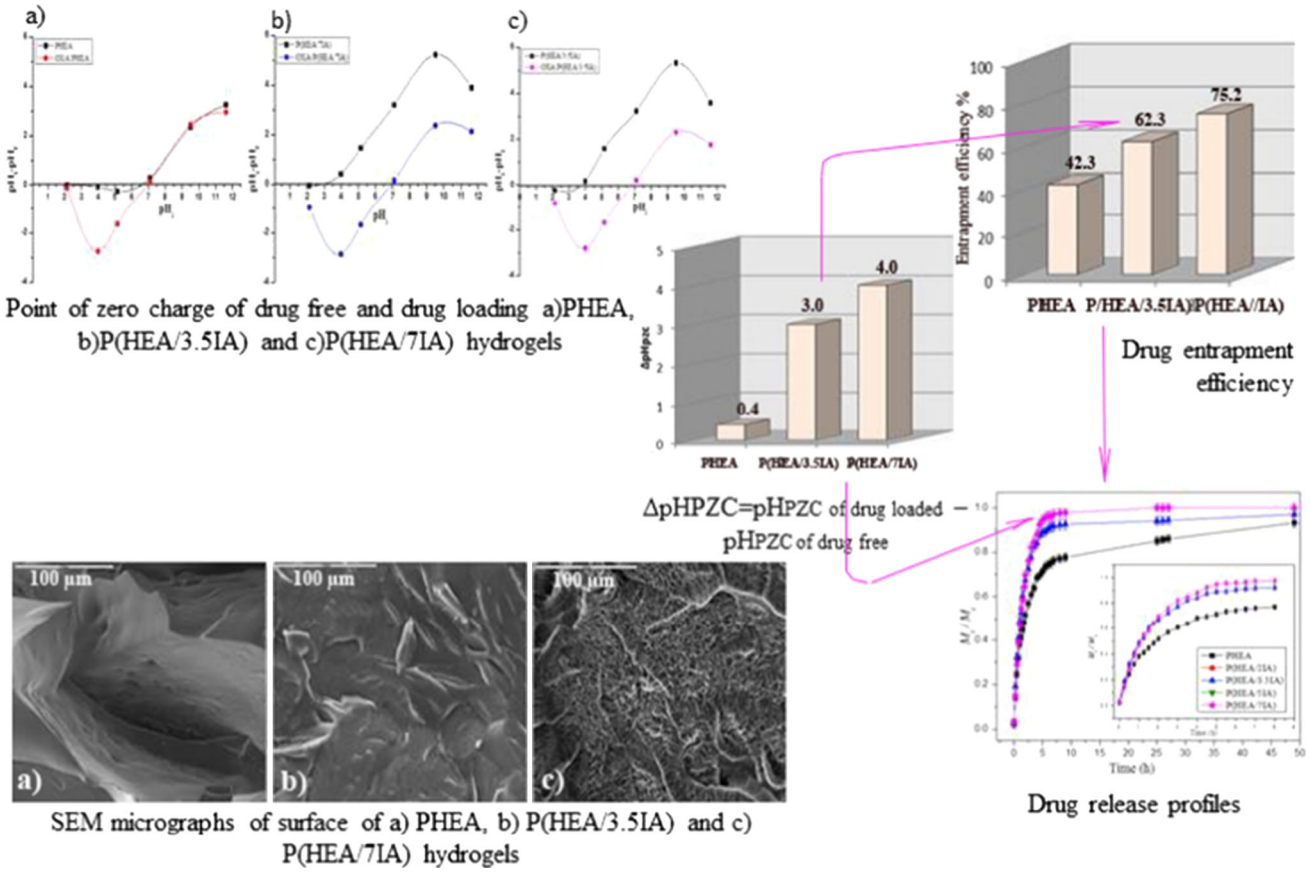

Scheme 3 Relation between surface charge, surface morphology, drug entrapment efficiency and drug release profiles of PHEA, P(HEA/3.5IA) and P(HEA/7IA)

Table 6 Parameters calculated from fitting release data by different kinetic models

	Mathematical model	Estimated parameters, SSR, AIC and R^2	Samples				
			PHEA	P(HEA/2IA)	P(HEA/3.5IA)	P(HEA/5IA)	P(HEA/7IA)
1.	Higuchi model	k_H	0.047	0.049	0.062	0.061	0.060
		SSR	0.003	0.006	0.004	0.005	0.012
		AIC	−62	−49	−42	−35	−33
		R^2	0.991	0.981	0.987	0.979	0.964
2.	Ritger–Peppas model	k_1	0.045	0.028	0.043	0.038	0.029
		n	0.505	0.619	0.582	0.614	0.670
		SSR	0.003	0.001	0.002	0.001	0.003
		AIC	−60	−66	−47	−48	−42
		R^2	0.990	0.997	0.993	0.995	0.989
3.	Peppas–Sahlin model	k_1	0.025	0.020	0.029	0.0236	0.013
		k_2	−0.001	−0.001	−0.001	−0.001	−0.001
		m	0.696	0.737	0.734	0.787	0.930
		SSR	0.001	0.001	0.001	0.001	0.001
		AIC	−69	−68	−47	−51	−47
		R^2	0.996	0.998	0.994	0.996	0.994
4.	Peppas–Sahlin model when $m = 0.5$	k_1	0.049	0.038	0.051	0.046	0.041
		k_2	−0.001	0.001	0.001	0.002	0.002
		SSR	0.003	0.002	0.002	0.002	0.004
		AIC	−64	−65	−45	−46	−45
		R^2	0.991	0.995	0.992	0.993	0.988

Drug loading and entrapment efficiency

The results for drug loading (DL, mg drug/g hydrogel) and entrapment efficiency (EE, %) of PHEA and P(HEA/IA) hydrogels are presented in Table 5. Hydrogels prepared without IA were able to load a small amount of OXA (22 ± 0.11 mg/g hydrogel, 42 ± 0.12 %) due to their low degree of swelling. Introducing IA into hydrogels, the swelling capacity becomes higher, and therefore it can absorb a higher amount of the drug. The higher q_e make easier the diffusion of the drug molecules through polymeric network, and at the same time, improves the incorporation of drug molecules into pores, resulting in a more efficient drug loading. The highest entrapment efficiency of OXA (75 ± 0.14 %) was achieved with P(HEA/7IA) hydrogel. These data suggest that hydrophobic drugs could be entrapped into PHEA and P(HEA/IA) hydrogels, and DL and EE could be adjusted by the swelling capacity of hydrogels, i.e. varying the IA content.

The in vitro release of OXA from PHEA and P(HEA/IA) hydrogels were investigated in pH buffers of 2.20 and 7.40, at 37 °C. We found that the low amount of OXA was released at acidic pH 2.20 (Fig. 8a) due to the low swelling capacity of hydrogels and the insolubility of OXA at acidic pHs. On the other hand, the higher amount of OXA was released in a pH of 7.40. The release profile data are presented in Fig. 8b.

As seen from Fig. 8b, significant differences in OXA released were observed between PHEA and P(HEA/7IA) hydrogels. The synthesized hydrogels showed sustained drug release up to 48 h, in a buffer pH of 7.40, at 37 °C. The release rate of OXA increased with increasing IA content. In a pH of 7.40, the OXA molecule (pK_a 4.3), and both carboxylic groups of IA are fully ionized. This leads to the mutual electrostatic repulsion, which facilitates the drug release. Therefore, a greater amount of oxaprozin was released faster from the network containing higher amount of IA.

As previously reported, the drug loaded amount may affect the drug release rate [57]. We found that the hydrogels loaded with a higher amount of OXA showed faster release. This phenomenon could be attributed to the change of the drug diffusivity caused by the different drug loading levels.

Also, we observed that all hydrogels exhibit fast release of OXA (of 40 and 50 %) in the initial period of release (2 h). After the initial "burst", OXA was released slowly, as a result of the swelling. Observed "burst" effect is caused by OXA adsorbed, or poorly entrapped at or near the surface of hydrogels. The relation between surface charge, surface morphology of hydrogels and their drug loading efficiency and release profiles are presented in Scheme 3.

PZC results confirm that the adsorption of drug on the surface of P(HEA/IA) hydrogels is greater than on the PHEA surface. This can be also explained by the surface morphology of P(HEA/IA) hydrogels which is wavy, coral-like texture, having a lot of microchannels. Such structure is suitable for the adsorption of higher amount of the drug compared to smooth surface of PHEA hydrogels. This was also confirmed by the initial "burst" for the drug release profiles, obtained in a pH of 7.40.

Analysis of the drug transport mechanism

In order to study the mechanism of the drug release from synthesized PHEA and P(HEA/IA) hydrogels, the in vitro obtained drug release data were fitted using four different kinetic models (Eqs. 6–9). Calculated parameters are presented in Table 6.

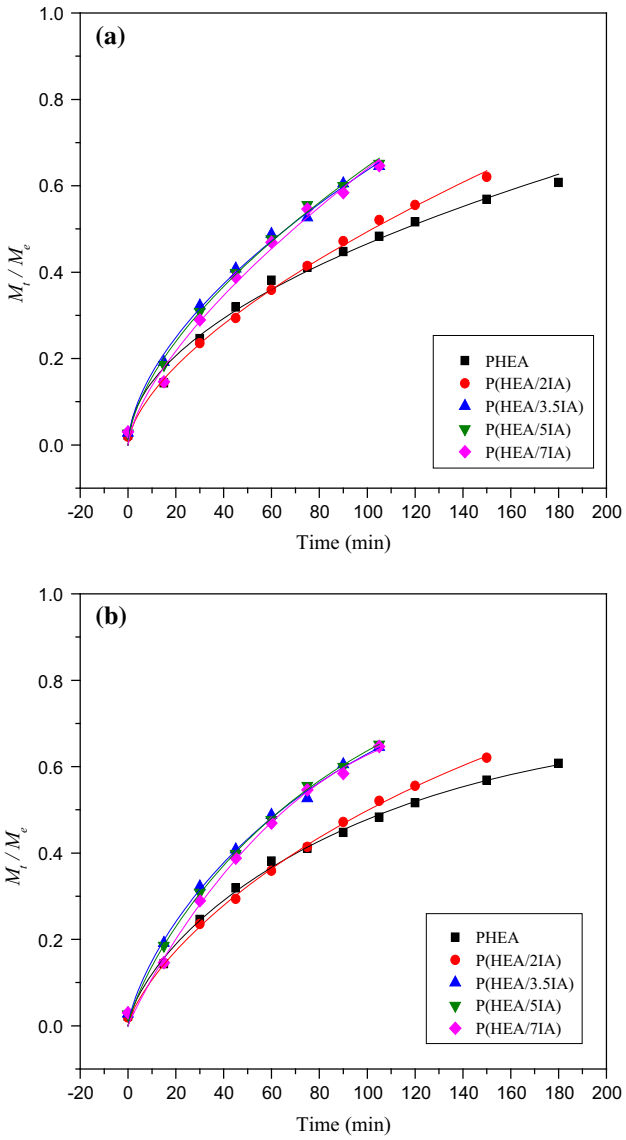

Fig. 9 In vitro drug release data fitted by **a** Ritger–Peppas and **b** Peppas–Sahlin models

Analysing of the Akaike information criterion (AIC) values, it turns out that Peppas–Sahlin and Ritger–Peppas models best describe release phenomena in the investigated drug/hydrogel systems. Figure 9a, b presents the fitting of the experimental plots by those two models.

The values of the exponent *n,* related to the drug transport mechanism, were calculated using the Ritger–Peppas model (Eq. 7). The obtained values of *n* (0.50 and 0.67) point out that the drug transport mechanism is Fickian diffusion for PHEA hydrogel, but anomalous for the hydrogels containing IA (Table 6).

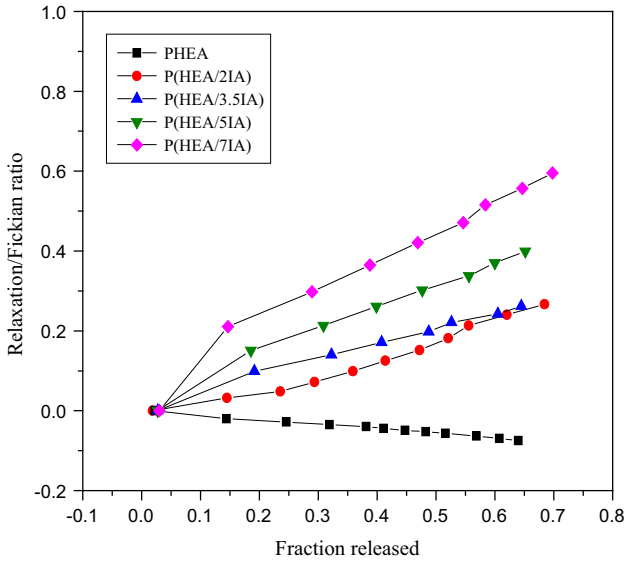

Fig. 10 The ratio *R/F* versus the fraction of the drug released from PHEA and P(HEA/IA) hydrogels

Using the Peppas–Sahlin equation Eq. 8 and the parameters estimated from Eq. 10, the ratio between the relaxation (*R*) and the diffusional (*F*) contribution during the drug release were calculated. The ratio *R/F* as a fraction of the drug released from the hydrogels is shown in Fig. 10. We found that the PHEA hydrogel shows lower *R/F* ratio than hydrogels containing IA. These results are another confirmation that the drug transport mechanism from P(HEA/IA) hydrogels is anomalous. It can be noted that the importance of the relaxation contribution for the drug release is more pronounced in the hydrogels containing itaconic acid compared to the PHEA hydrogel.

Antibacterial activity

The antibacterial activity of hydrogels is very valuable property for variety of biomedical applications [58, 59]. Bacterial infections associated with medical devices have not been eradicated, despite advanced sterilization and aseptic techniques. Antibacterial activity of drug-free and drug-loaded hydrogels with different content of IA (0, 2 and 7 mol%) were determined against *E. coli* and *S. aureus.* The zone of inhibition test was performed as a preliminary step to screen those systems for the antimicrobial activity. As seen from Fig. 11, the inhibition of bacterial cell growth was observed only in contact with the sample. The presence of the drug into hydrogel composition did not show an additional effect on their antibacterial activity.

Conclusions

The series of dual stimuli-sensitive anionic copolymeric hydrogels containing HEA and IA were successfully

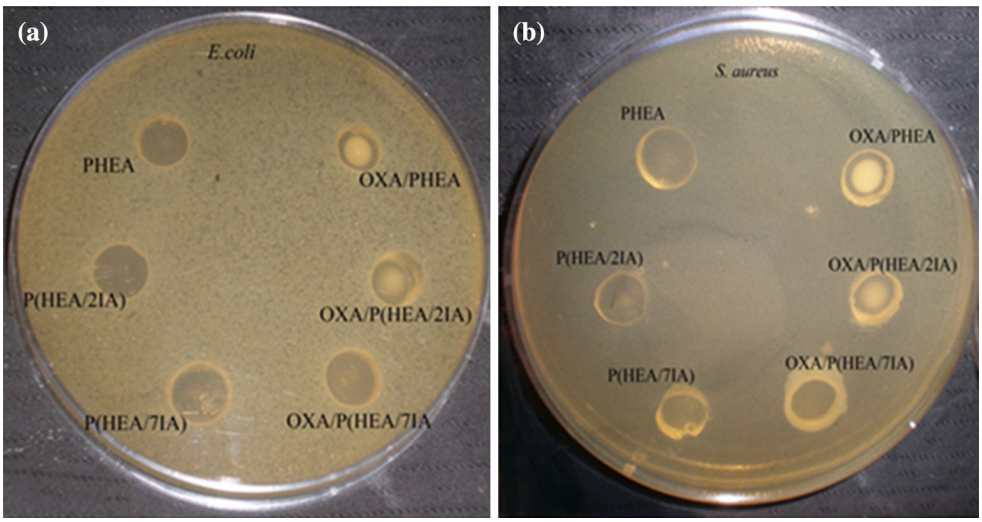

Fig. 11 Zone of inhibition test of antimicrobial activity of PHEA, P(HEA/2IA), P(HEA/7IA), OXA/PHEA, OXA/P(HEA/2IA) and OXA/P(HEA/7IA) hydrogels against **a** *E. coli* and **b** *S. aureus*

synthesized by the free-radical crosslinking copolymerization, and tested as matrices for the controlled release of a hydrophobic drug, Oxaprozin. The chemical composition of hydrogels and successful incorporation of the drug within hydrogels were confirmed by FTIR spectra. The SEM micrographs of hydrogels revealed porous interior structure which was transformed to less porous with loading of the drug. The T_g values of drug-free copolymers were observed in range of 15–34 °C and for drug loaded were in range of 20–45 °C.

Swelling studies conducted in pH physiological range (2.20–8.00) and the temperature range from 25 to 50 °C, showed robust pH- and temperature-sensitive behavior, which classifies them into ''smart'' polymeric biomaterials. The VPPTs of the P(HEA/IA) hydrogels detected by their swelling behavior, are in physiologically relevant temperature range of 37–40 °C. This phenomenon makes them suitable for the site-specific drug delivery using changes in temperature as a trigger.

In vitro drug release study conducted in a pH of 2.20 and 7.40, at 37 °C shows pH-sensitive delivery. The obtained release profiles for OXA, in a pH 7.40, indicate that the release rate of the drug could be effectively controlled by modifying the composition of the hydrogels.

Antibacterial activity of the hydrogels was examined against *E. coli* and *S. aureus*. Our data showed that both in drug-free and drug-loaded hydrogels the number of bacterial cells were slightly reduced, with no additional benefit of the OXA present.

Based on all these unique properties, it could be concluded that these novel hydrogels have a great potential to be used as the site-specific drug delivery systems. Such medical applications may include, for instance, cases where certain drugs are unstable in harsh gastric conditions, or drugs which manifest their side effects in the upper gastrointestinal tract. These systems could be also of a great interest in clinical trials to improve therapeutic efficacy and patient compliance, and to help reducing the potential side effects of a drug.

Acknowledgements This work has been supported by the Ministry for Education, Science and Technological Development of the Republic of Serbia (Grants No 172062 and 172026).

References

1. Jaiswai M, Koul V (2013) Assessment of multicomponent hydrogel scaffolds of poly(acrylic acid-2-hydroxy ethyl methacrylate)/gelatin for tissue engineering applications. J Biomater Appl 27:848–861
2. Yin W, Su R, Qi W, He Z (2012) A casein-polysaccharide hybrid hydrogel cross-linked by transglutaminase for drug delivery. J Mater Sci 47:2045–2055. doi:10.1007/s10853-011-6005-7
3. Saraydin D, Karadag E, Sahiner N, Guven O (2002) Incorporation of maleic acid into acrylamide hydrogel by radiation technique and its effect on swelling behavior. J Mater Sci 37:3217–3223. doi:10.1023/A:1016170630750
4. Peppas NA, Bures P, Leobandung W, Ichikawa H (2000) Hydrogels in pharmaceutical formulations. Eur J Pharm Biopharm 50:27–46
5. Park K, Shalaby WSW, Park H (1991) Biodegradable hydrogels for drug delivery, Technomic Publishing Company Inc, Lancaster
6. Lee KY, Mooney DJ (2001) Hydrogels for tissue engineering. Chem Rev 101:1869–1879
7. Kashyap N, Kumar N, Kumar MN (2005) Hydrogels for pharmaceutical and biomedical applications. Crit Rev Ther Drug 22:107–149
8. Khademhosseini A, Langer R (2007) Review: microengineered hydrogels for tissue engineering. Biomaterials 28:5087–5092
9. Koh MY, Ohtsuki C, Miyazaki T (2011) Modification of polyglutamic acid with silanol groups and calcium salts to induce calcification in a simulated body fluid. J Biomater Appl 25:581–594
10. Jaiswal M, Gupta A, Dinda AK, Koul V (2010) Polycaprolactone diacrylate (PCL-DAr) crosslinked biodegradable semi-interpenetrating networks (semi-IPNs) of polyacrylamide and gelatin for controlled drug delivery. Biomed Mater 5:065014
11. He H, Cao X, Lee LJ (2004) Design of a novel hydrogel-based intelligent system for controlled drug release. J Control Release 95:391–402
12. Vihola H, Laukkanen A, Hirvonen J, Tenhu H (2002) Binding and release of drugs into and from thermosensitive poly(*N*-vinyl caprolactam) nanoparticles. Eur J Pharm Sci 16:69–74
13. Young KC, Seo YJ, Young HK (1992) A glucose-triggered solubilizable polymer gel matrix for an insulin delivery system. Int J Pharm 80:9–16
14. Shamunga Sudar S, Sangeetha D (2012) Investigation on sulphonated PEEK beads for drug delivery, bioactivity and tissue engineering applications. J Mater Sci 47:2736–2742. doi:10.1007/s10853-011-6100-9
15. Liu C, Yu J, Jiang G, Liu X, Li Z, Gao G, Liu F (2013) Thermosensitive poly(*N*-isopropylacrylamide)hydrophobic associated hydrogels: optical, swelling/deswelling, and mechanical properties. J Mater Sci 48:774–784. doi:10.1007/s10853-012-6794-3
16. Burugapalli K, Bhatia D, Koul V, Choudhary V (2010) Interpenetrating polymer networks based on poly(acrylic acid) and gelatin I: swelling and thermal behavior. J Appl Polym Sci 82:217–227
17. Bajpai AK, Shukla SK, Bhanu S, Kankane S (2008) Responsive polymers in controlled drug delivery. Prog Polym Sci 33:1088–1118
18. Mohamed R, Choudhary V, Koul V (2009) Synthesis and characterization of biodegradable interpenetrating polymer networks based on gelatin and divinyl ester synthesized from poly(caprolactone diol). J Appl Poly Sci 111:1478–1487
19. Ekici S (2011) Intelligent poly(*N*-isopropylacrylamide)-carboxymethyl cellulose full interpenetrating polymeric networks for protein adsorption studies. J Mater Sci 46:2843–2850. doi:10.1007/s10853-010-5158-0
20. Kim JK, Kim HJ, Chung JY, Lee JH, Young SB, Kim YH (2013) Natural and synthetic biomaterials for controlled drug delivery. Arch Pharm Res 37:60–68
21. Khutoryanskaya OV, Mayeva ZA, Mun GA, Khutoryanskiy VV (2008) Designing temperature-responsive biocompatible copolymers and hydrogels based on 2-hydroxyethyl(meth)acrylates. Biomacromolecules 9:3353–3361
22. Chan Y, Wong T, Byrne F, Kavallaris M, Bulmus V (2008) Acid-labile core cross-linked micelles for pH-triggered release of antitumor drugs. Biomacromolecules 9:1826–1836

23. Arun A, Reddy BSR (2005) In vitro drug release studies from the polzmeric hydrogels based on HEA and HPMA using 4-{(*E*)-[(3*Z*)-3-(4-(acryloxy)benzylidene)-2-hexylidene]methyl}phenyl acrylate as a crosslinker. Biomaterials 26:1185–1193
24. Luck M, Paulke BR, Schroder W, Blunk T, Muller RH (1998) Analysis of plasma protein adsorption on polzmeric nanoparticles with different surface characteristics. J Biomed Mater Res 39:478–485
25. McAllister K, Sazani P, Adam M, Cho MJ, Rubinstein M, Samulski RJ, DeSimone JM (2002) Polzmeric nanogels produced via inverse microemulsion polymerization as potential gene and antisense delivery agents. J Am Chem Soc 124:15198–15207
26. Ramos CM, Lainez S, Sancho F, Esparza MAG, Planells-Cases R, Verdugo JMG, Ribelles JLG, Sanchez MS, Pradas MM, Barcia JA, Soria JM (2008) Differentiation of postnatal neural stem cells into glia and functional neurons on laminin-coated polymeric substrates. Tissue Eng A 14:1365–1375
27. Lluch AV, Fernandez AC, Ferrer GG, Pradas MM (2009) Bioactive scaffolds mimicking natural dentin structure. J Biomed Mater Res B 90:182–194
28. Hoogenboom R, Popescu D, Steinhauer W, Keul H, Moller M (2009) Nitroxide-mediated copolymerization of 2-hydroxyethyl acrylate and 2-hydroxypropyl acrylate: copolymerization kinetics and thermoresponsive properties. Marcromol Rap Commun 30:2042–2048
29. Krezović BD, Dimitrijević SI, Filipović JM, Nikolić RR, Tomić SLj (2013) Antimicrobial P(HEMA/IA)PVP semi-interpenetrating network hydrogels. Polym Bull 70:809–819
30. Dobić SN, Filipović JM, Tomić SLj (2012) Synthesis and characterization of poly(2-hydroxyethyl methacrylate/itaconic acid/poly(ethylene glycol)dimethacrylate)hydrogels. Chem Eng J 179:372–380
31. Rainsford KD, Omar H, Ashraf A, Hewson AT, Bunning RAD, Rishiraj R, Shepherd R, Seabrook W (2002) Recent pharmacodynamics and pharmacokinetic findings on oxaprozin. InflammoPharmalogy 10:185–239
32. Henry DA (1988) Side effects of non-steroidal anti-inflammatory drugs. Bailliere Clin Rheum 2:425–454
33. Mau S, Lovely G, Prakash KS, Punit K, Sujata S, Tej PS (2013) Current perspectives in NSAID-induced gastropathy. Mediat Inflamm. doi:10.1155/20137258209
34. Yazdanian M, Briggs K, Jankovsky C, Hawi A (2004) The high solubility definition of the current FDA guidance on biopharmaceutical classification system may be too strict for acidic drugs. Pharmacol Res 21:293–299
35. Brown K (1971) Oxazoles, US patent 3,578,671
36. Božić B, Rogan J, Poleti D, Božić B, Uščumlić G (2012) Synthesis, characterization and antiproliferative activity of transition metal complexes with 3-(4,5-diphenyl-1,3-oxazol-2-yl)propanoic acid (oxaprozin). Chem Pharm Bull 60:865–869
37. Mall ID, Srivastava VC, Kumar GVA, Mishra IM (2006) Characterization and utilization of mesoporous fertilizer plant waste carbon for adsorptive removal of dyes from aqueous solution. Colloid Surface A 278:175–187
38. Bell CL, Peppas NA (1995) Measurement of swelling force in ionic polymer networks. III. Swelling force of interpolymer complexes. J Control Release 37:277–280
39. Peppas NA (1985) Analysis of Fickian and non-Fickian drug release from polymer. Pharm Acta Helv 60:110–111
40. Elechiguerra JL, Burt JL, Morones JR, Camacho-Brabado A, Gao X, Lara HH, Yacaman MJ (2005) Interaction of silver nanoparticles with HIV-1. J Nanobiotechnol 3:1–10
41. Harland RS, Peppas NA (1987) Solute diffusion in swollen membranes. Polym Bull 18:553–556
42. Wu CL, He H, Gao HJ, Liu G, Ma RJ, An YL, Shi LQ (2010) Synthesis of Fe_3O_4[SiO_2]polymer nanoparticles for controlled drug release. Sci China Chem 53:514–518
43. Higuchi T (1963) Mechanism of sustained-action medication: theoretical analysis of rate of release of solid drugs dispersed in soled matrices. J Pharm Sci 52:1145–1148
44. Peppas NA, Sahlin JJ (1989) A simple equation for the description of solute release III. Coupling of diffusion and relaxation. Int J Pharm 57:169–172
45. Yamoaka K, Nakagawa T, Uno T (1978) Application of the Akaike information criterion (AIC) in the evaluation of linear pharmacokinetics equations. J Pharmacokinet Biopharm 6:165–175
46. Tomić SLj, Dimitrijević SI, Marinković AD, Najman S, Filipović JM (2009) Synthesis and characterization of poly(2-hydroxyethyl methacrylate/itaconic acid) copolymeric hydrogels. Polym Bull 63:837–851
47. Seda GS, Asli E (2010) Theoretical and vibrational studies of 4,5-diphenyl-2-2 oxazole propionic acid (oxaprozin). Spectrochim Acta A 75:1370–1376
48. Wang XF, Sun XW, Liu WX, Gong BY, Gao NB (2008) Chitosan hydrogel beads for fulvic acid adsorption: behaviors and mechanisms. Chem Eng J 142:239–247
49. Pechenyuk SI (1999) The use of the pH at the point of zero charge for characterizing the properties of oxide hydroxides. Russ Chem B 48:1017–1023
50. Asmarandei I, Fundueanu G, Cristea M, Harabagiu V, Constantin M (2013) Thermo- and pH.sensitive interpenetrating poly(*N*-isopropylacrylamide)/carboxymethyl pullulan network for drug delivery. J Polym Res 20:293–306
51. Alvarez-Lorenzo C, Concheiro A (2002) Reversible adsorption by a pH- and temperature-sensitive acrylic hydrogel. J Control Release 80:247–257
52. Wang Y, Yuan ZC, Chen DJ (2012) Thermo- and pH-sensitive behavior of hydrogels based on oligo(ethylene glycol) methacrylates and acrylic acid. J Mater Sci 47:1280–1288. doi:10.1007/s10853-011-5901-1
53. Ritger PL, Peppas NA (1987) A simple equation for description of solute release I. Fickian and non-Fickian release from non-swellable devices in the form of slabs, spheres, cylinders or discs. J Control Release 5:23–36
54. Caykara T, Dogmus M, Kantoglu O (2004) Network structure and swelling-shrinking behaviors of pH-sensitive poly(acrylamide-co-itaconic acid) hydrogels. J Polym Sci Pol Phys 42:2586–2594
55. Canal T, Peppas NA (1989) Correlation between mesh size and equilibrium degree of swelling of polymeric networks. J Biomed Mater Res 23:1183–1193
56. Gudeman LF, Peppas NA (1995) pH-sensitive membranes from poly (vinyl alcohol)/poly (acrylic acid) interpenetrating networks. J Membr Sci 107:239–248
57. Ruan G, Feng SS (2003) Preparation and characterization of poly(lactic-acid)-poly(ethylene glycol)-poly(lactic acid)(PLA-PEG-PLA) microspheres for controlled release of paclitaxel. Biomaterials 24:5037–5044
58. Yu H, Xu X, Chen X, Lu T, Zhang P, Jing X (2007) Preparation and antibacterial effects of PVA–PVP hydrogels containing silver nanoparticles. J Appl Polym Sci 103:125–133
59. Martineau L, Shek PN (2006) Evaluation of a bi-layer wound dressing for burn care: II In vitro and in vivo bactericidal properties. Burns 32:172–179
60. Kruszewska H, Zareba T, Tyski S (2002) Search of antimicrobial activity of selected non-antibiotic drugs. Acta Pol Pharm 59:463–469
61. Peppas NA, Buri PA (1985) Surface, intrerfacial and molecular aspects of polymer bioadhesion on soft tissues. J Control Release 2:257–275